Nitrogenation and sintering of (Nd-Zr)Fe10Si2 tetragonal compounds for permanent magnets applications

J. M. Barandiaran, A. Martin-Cid, A. M. Schönhöbel, J. S. Garitaonandia, M. Gjoka, D. Niarchos, S. Makridis, Oleksandr Pasko, Alex Aubert, F. Mazaleyrat, et al.

Nitrogenation and sintering of (Nd-Zr)Fe10Si2 tetragonal compounds for permanent magnets applications

J M Barandiaran[1,2], A Martin-Cid[1], AM Schönhöbel[1], J S Garitaonandia[2] M Gjoka[3], D Niarchos[3], S Makridis[4], A Pasko[5], A Aubert[5], F Mazaleyrat[5] and G Hadjipanayis[6]

[1] Basque Center for Materials, Applications and nanostructures (BCMaterials), Leioa, Spain

[2] University of the Basque Country (UPV/EHU), Leioa, Spain

[3] NCSR Demokritos, Athens, Greece

[4] University of Patras, Patras, Greece

[5] Laboratoire SATIE, ENS Paris-Saclay, Cachan, France

[6] University of Delaware, Newark, DE, USA

Abstract: Nd-xZrxFe10Si2 alloys have been prepared in the tetragonal ThMn12-type structure by arc-melting and melt spinning and then nitrogenated to improve their magnetic properties. For x = 0.4 and 0.6 the Curie temperature and magnetic anisotropy fields increases from 280-300 ºC to about 390 ºC and from 2.8-3 Tesla to 4.5-5 Tesla respectively. The saturation magnetization remains almost unchanged. The nitrogenated powders were processed by Spark Plasma Sintering (SPS) leading to compact pellets, which retain the full Nitrogen content and magnetic properties up to 600ºC, but segregated Fe-Si at elevated temperatures. Nitrogenation and SPS processing are, therefore, appropriate for sintering metastable materials such as (NdZr)Fe10Si2 into compact material without loosing functional properties. This opens a way towards a new family of permanent magnets, lean of critical raw materials.

Introduction:

The critical and strategic character of rare earth (R) elements as raw materials [1] has motivated an extensive search of new rare-earth-lean and rare-earth-free compounds for permanent magnets, which could substitute $Nd_2Fe_{14}B$ in some applications not demanding a high performance [2] In particular, a renewed interest in the tetragonal $R(Fe,M)_{12}$ compounds, with the $ThMn_{12}$ structure (1:12 for short) has recently arisen. Here M is a transition metal or other element stabilizing the 1:12 structure. These compounds were studied in the 90's [3-5] and are rare-earth-lean with room-temperature ferromagnetism and a large uniaxial magneto-crystalline anisotropy in some of them. Among them, special attention has been paid to those with light rare earths as cerium, the most abundant and least critical rare earth [6-10], and praseodymium and neodymium. The need of a stabilizing element, M, in the Fe lattice, usually has a harmful effect in the magnetization and Curie temperature of such compounds, so there are intense efforts to reduce its content to a minimum. However, Zhou et al. [7] reported an unexpectedly high Curie temperature T_c in $CeFe_{10}Si_2$ with 2 atoms of stabilizing Si. Both old

[11-13] and very recent studies [14-16] confirm the stability of the tetragonal RFe10Si2 structures only for the rare-earth R (and other metals) having an atomic radius equal or smaller than 0.181 nm, such as Sm and heavier Rare Earths as well as Zr and Hf. In fact, $CeFe_{10}Si_2$ and Nd $Fe_{10}Si_2$ have not the 1:12 structure but the Th_2Zn_{17} (2:17). Sakurada et al. [17] proposed that the stability of the 1:12 structure in the $R(Fe,Si)_{12}$ alloys depends on the average radius of the atoms in the R sites (the 2a sites). The stabilization of the 1:12 structure occurs when part of the larger atoms in the $RFe_{10}Si_2$ is replaced with smaller Zr atoms. The 1:12- structure-stabilizing effect of Zr is evident even in the case of Sm, which has the limit atomic radius of 0.181 nm for a stable compound.

In $(Ce\text{-}Zr)Fe_{10}Si_2$, the effect of Ce substitution on the parent $ZrFe_{10}Si_2$ promotes a moderate increase (up to 0.5 Tesla) of the magnetic anisotropy field, but also destabilizes the 1:12 structure [14]. Ce is an intermediate valence element with very low or no magnetic moment at all, and its effect has been traced to a pure geometrical distortion of the lattice [15].

$(Nd\text{-}Zr)Fe_{10}Si_2$ display improved magnetic properties and anisotropy with respect to Ce compounds [16]. As seen in fig. 1, best properties are achieved around $Nd_{0.5}Zr_{0.5}$. However, Nd-Fe compounds have usually a planar anisotropy and are not suitable for PM applications. Mössbauer spectra of aligned samples of the Zr = 0.4, 0.6, and 0.8 compounds indicate the anisotropy has a conical alignment, i.e., is between planar and uniaxial.

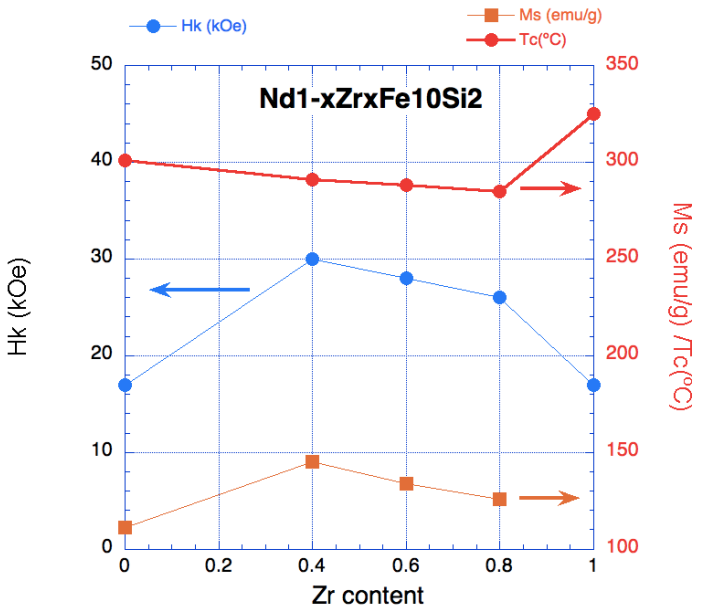

Figure 1.- *Magnetic properties of $Nd_{1-X}Zr_XFe_{10}Si_2$ (data from reference[16])*

The way to turn planar anisotropy into axial and to enhance magnetic performance of Nd compounds is the insertion of a light element (such as B in the well known Nd2Fe12B magnets) into the lattice. Introducing interstitial N into the 2b site of the crystal lattice has a similar effect. Nitride formation is a quite difficult task for NdFe10Si2 and a number of trials have been carried out in this work, until successful nitrogenation. The nitrides, however, decompose at high temperature (>550ºC) making nearly impossible the sintering of bulk magnets. In this work, we report our successful experiments to nitrogenate the NdFe10Si2 compound using high pressures. We also report the use of a very fast sintering technique: spark plasma sintering (SPS) for preparing bulk (Zr-Nd)$Fe_{10}Si_2$(N) pellets, and show the initial 1:12 nitrogenated phase is stable for treatments up to 600ºC, providing a way to produce sintered magnets out of the nitrogenated powders. SPS has been successfully used for sintering ferrites [18], $Nd_2Fe_{14}B$ [19] and Sm-Co magnets [20], and recently for (Ce-Nd)(Fe-Mo)N 1:12 compounds [21]

Experimental

Samples were prepared by arc melting pure constituents (purity better tahn 99.9%) and milled to an average grain size of about 10 μm in a ball mill. Some alloys were further melt spun before milling to a similar grain size. Nitrogenation was performed in a High Pressure Volumetric Sorption Analyzer reactor (HIPVM-160) under pressures up to 20 bar and temperatures up to 550ºC. SPS was performed in a SPSS, DR. SINTER LAB Apparatus, located at the ICMPE Laboratory in Thiais, France.

XRay diffraction (XRD) patterns were obtained by means of different diffractometers at the different laboratories in which this study has been performed. SIEMENS D500 and Philips X-pert diffractometers, using Cu-Kα radiation, were used in Demokritos National Research Center (Athens, Greece) and in BCMaterials-UPV/EHU (Leioa, Spain) respectively. A Bruker D2 Phaser with Co-Kα radiation was used instead at the ENS Paris-Saclay, in Cachan, France. Magnetic measurements were carried out in a magnetic TGA for determining the Curie temperatures and any phase change during heating. A 2 Tesla electromagnet VSMs (Lake Shore 7400 and Microsense EZ-7) and a superconducting coil magnetometer (Quantum Design) in 7 Tesla applied field were used for magnetization vs. field, M(H), measurements. The oriented powder samples used in some magnetic measurements were prepared by dissolving the powder in molten wax or a polymeric resin under a magnetic field of about 1 Tesla and waiting for solidification or curing, respectively.

Mössbauer was performed at room temperature in a constant acceleration spectrometer with transmission geometry, using a Co(Rh) source calibrated with an iron foil. Scanning Electron Microscopy (SEM) was performed in a desktop Phenom ProX at Demokritos (Athens).

Results and discussion

a) Nitrogenation

Nitrogen is known to enter into the 1:12 lattice and occupy the 2b interstitial site [22-23], and recently reported studies on (Ce-Nd)$(Fe\text{-}Mo)_{12}$ demonstrate the increase of the Curie Temperature, the magnetization and coercivity [24]. However, no nitrogenation of Si containing 1:12 R-Fe phases has been reported up to now. Samples from two compositions and different preparation process were used for nitrogenation (table 1). The $Nd_{0.6}Zr_{0.4}Fe_{10}Si_2$ compounds were prepared by arc-melting and milled to an average grain size of about 10 μm in a ball mill. The $Nd_{0.4}Zr_{0.6}Fe_{10}Si_2$ were melt-spun after arc-melting and before milling. All compounds show the 1:12 structure with small amounts of bcc Fe-Si. Nitrogenation was performed in a High Pressure Volumetric Sorption Analyzer reactor (HIPVM-160) under pressures up to 20 bar and temperatures up to 550ºC. Results are summarized in table 1. For the $Nd_{0.6}Zr_{0.4}Fe_{10}Si_2$ compound (samples P1-P3) several optimization studies that included increasing temperature, and time and pressure, gave increasing amounts of the nitrogentaed 1:12 phase, but never reached the 100% value. Another approach was therefore tried in $Nd_{0.4}Zr_{0.6}Fe_{10}Si_2$that involved melt spinning and milling of the melt spun ribbons to a similar average grain size (sample A1). The grain size dispersion, however, was lower than in the former case, and 100% nitrogenation of the 1:12 phase is reached at relatively low temperature for long treatments at high pressure. The amount of Fe-Si phase present in the original compound slightly increased along the nitrogenation process.

Table 1.- *$(Nd\_Zr)Fe_{10}Si_2$ Nitrogenation process*

Nº	Composition	Processing	1:12 lattice		Nitride lattice		1:12/nitride/ α-Fe-Si fraction
			a (nm)	c (nm)	a (nm)	c (nm)	
P1 [a]	**$Nd_{0.6}Zr_{0.4}Fe_{10-2}$**	400ºC /4h / 7 bar	0.8410	0.4745	0.8500	0.4742	65 / 28 / 7
P2 [a]	"	500ºC /3h / 20 bar	0.8409	0.4742	0.8494	0.4746	59 / 36 / 5
P3 [a]	"	550ºC /18h / 20 bar	0.8411	0.4746	0.8500	0.4746	21 / 71 / 7
A1 [b]	**$Nd_{0.4}Zr_{0.6}Fe_{10}Si_2$**	450ºC /24h / 20 bar	0.8370 [c]	0.4737 [c]	0. 8500	0.4739	- / 89 / 11

[a] Arc melted; [b] Melt spun, [c] Taken from ref [16]

The effects of nitrogenation have been studied by XRD, Mossbauer Spectroscopy, SEM and magnetic measurements. The XRD patterns of the nitrogenated powders show the presence of the 1:12 and bcc FeSi phases, as in the non-nitrogenated ones. No new phases appear after the treatment. This is further confirmed by Mössbauer spectroscopy (see below). The peaks of the

1:12 phase are displaced with respect to and broader than those of the non-nitrogenated. A pattern of the $Nd_{0.4}Zr_{0.6}Fe_{10}Si_2$ nitrogenated powders can be seen in Figure 7, where it is labeled as "starting powder" for the SPS treatments. The non-nitrogentaed XRD patterns are displayed in reference [16]. Displacement of the peaks corresponds to the changes in lattice constants of the 1:12 phase, which are recorded in table 1. Broadening of the peaks could be attributed either to a substantial decrease of the grain size (below 100 nm) or to internal stresses which deform the lattice. Which of the two is correct is difficult to analyze from XRD alone. We have also performed SEM observations in the powders before and after nitrogenation. Pictures in Figure 2 show that the grain size and morphology are the same after nitrogenation, ruling out the decrease of grain size below 100 nm. On the other hand completely uniform nitrogenation is not expected to induce large stresses in the lattice. A possible explanation of the peak broadening is, therefore, the existence of a nitrogenation gradient inside the grains. This is quite probable because diffusion of nitrogen proceeds from the surface to the interior of the grains.

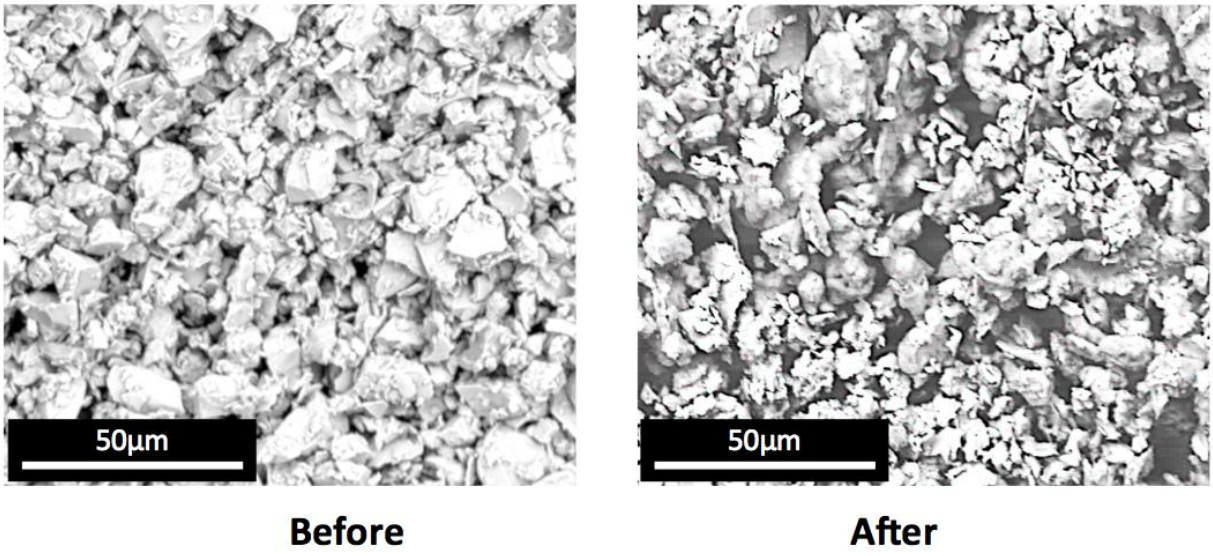

Figure 2.- *SEM pictures of the $Nd_{0.4}Zr_{0.6}Fe_{10}Si_2$ powders before and after nitrogenation.*

Nitrogen is shown to expand the crystal lattice by about 2-3% in volume, mainly by an increase of the parameter *a* of the unit cell (table 1), and to increase the Curie temperature (Tc) and magnetic anisotropy. Figure 3 clearly indicates the increase in Curie temperature and anisotropy field. The amount of Nitrogen entering the lattice can be estimated by the volume expansion and the increase of the Curie temperature [22-23]. In the case of $Nd_{0.6}Zr_{0.4}Fe_{10}Si_2$, which is only partially nitrogenated, we estimated 1 N atom/f.u. (2% volume and about 70ºC increase of Tc) and for $Nd_{0.4}Zr_{0.6}Fe_{10}Si_2$, the estimation is 1.5 N atoms (3% volume and 100ºC increase of Tc). The TGA (Figure 3 left) shows the apparent weight loose at the magnetic

transitions of the pure phase (300ºC) and the nitrogenated phase (369ºC). Further temperature increase reveals a decrease of weight (starting from below 500ºC and extending to about 700ºC), produced by the loss of nitrogen, and the segregation of more stable phases, which eventually result in a Tc around 760ºC. This can correspond to the appearance of a Fe rich compound, with some dissolved Si in it, as the Fe-Si phase already present in as prepared samples. This is further confirmed by XRD on the sintered samples (see below). For the fully nitrogenated sample A1, there is only a Tc (at about 383ºC), in the range 200-500ºC (see figure 5, below). The increase of Tc by about 100ºC is a major improvement of the magnetism in these phases, upon nitrogenation. The magnetic transition of the nitrogenated sample appears much broad than in the as prepared one (fig.5). This can be due to a dispersion in the amount of nitrogenation between different grains or even inside each of the grains.

The saturation magnetization is obtained from the extrapolation of M vs. $1/H^2$. It remains constant, or even decreases for the partially nitrogenated samples, but shows more than 5% increase (from 134 to 141 Am^2/kg) in the fully nitrogenated sample A1.

As disclosed in ref [16], oriented powder Mössbauer spectroscopy reveals a conical easy direction of the magnetization with aperture of 43º and 24º deg. for the compounds with Zr = 0.4 and 0.6, respectively. The conical easy direction requires a negative K_1 constant and a value of the second order anisotropy constant: $K_2 \geq |K_1|/2$. After full nitrogention, XRD of oriented powder of the Zr = 0.6 sample shows a fully uniaxial character, i.e $K_1 \geq 0$. Anisotropy field increases drastically even in partially nitrogenated samples: from 3 T to 5.3 T (77%) in P2 sample (36% nitride) and from 2.8 T to 4.5 T (61%) in A1 (100% nitride). The fully uniaxial character and the increase in the anisotropy field make these compounds very likely candidates for a new generation of RE lean permanent magnets. The curved shape of the perpendicular magnetization in oriented powder samples (figure 3 right) indicates, however, a large contribution of the second order anisotropy constant, which can be fitted to a value similar to K_1. Both constants are in the range of 600-700 $kJ.m^{-3}$ (see the complementary material of this work).

It must be noted that the grain size of the powder (above 10 μm) is very large to develop any appreciable coercivity, as would be expected for anisotropy fields around 5 Tesla. The nitrogenated powder of $Nd_{0.4}Zr_{0.6}Fe_{10}Si_2$ (A1) has a coercivity of only 22 mTesla.

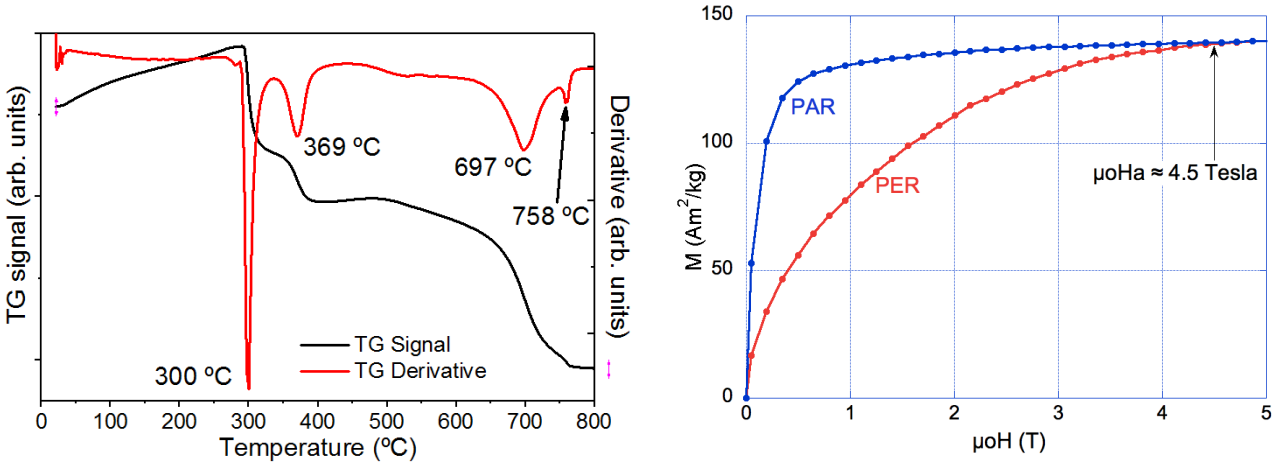

Figure 3.- *Magnetism of Nitrogenated samples: Left Magnetic TGA of a 36% nitrogenated sample (P2 in table 1) showing the original Tc (300ºC) and that of the nitrogenated phase (369ºC). Right: Parallel (PAR) and perpendicular (PER) magnetization of field oriented powders of the* $Nd_{0.4}Zr_{0.6}Fe_{10}Si_2$ *full nitride phase (sample A1). An increase of the saturation magnetization from 134 to 141* Am^2/kg*, and of the anisotropy field (*$\mu_0 Ha$*) from 2.8 to about 4.5 Tesla is achieved.*

Room Temperature (RT) Mössbauer spectra of the full nitrogenated sample (A1) is shown in Figure 4. The analysis of the spectra was performed using 3 different Fe sites (8i, 8j and 8f) in the 1:12 lattice and two different sites Fe sites for a bcc solid solution of Fe-Si, as in ref [16]. The Si content in this phase is assumed to be around 4%, as corresponds to the Curie temperature about 758ºC found in MTGA (Figure 2) [24]. The fitting also gives an average <Bhf>≈ 31.8 T for the Fe-Si phase (table 2), which is consistent with <Bhf> ≈ 32 Tesla, for 4.5% Si in Fe [25]. The two spectra of the Fe-Si phase correspond to the case of a Fe atom surrounded by 8 Fe atoms (A8) and the case in which Fe is surrounded by 7 Fe atoms and 1 Si atom (A7). Other possible Si concentrations around Fe are extremely improbable, according to the Poisson distribution for this Si content, and were not taken into account. The percentage of Fe atoms in the Fe-Si phase given by the Mössbauer is about 11%, slightly smaller than the XRD value (12%), and somewhat greater than before nitrogenation (8% by XRD)[16].

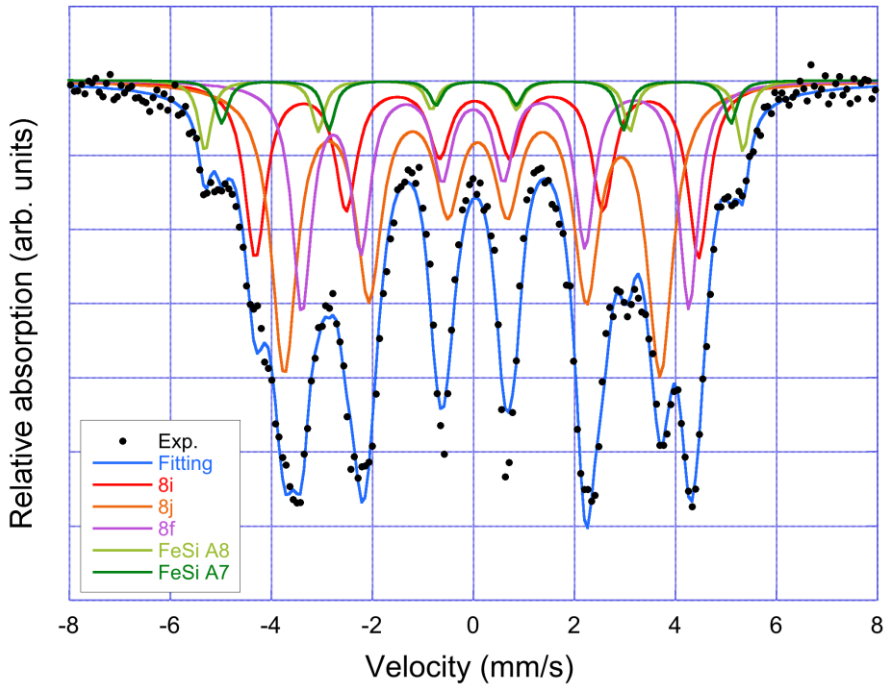

Figure 4.- *Room temperature Mössbauer spectrum of the fully nitrogenated sample A1. Three sites in the 1:12 structure and two in the bcc Fe-Si solid solution subspectra are shown.*

Fitting of the spectra for the 1:12 phase (table 2) disclose an increase of the hyperfine field (Bhf) of about 10% in the 8i and 8j Fe sites, and changes in the Quadrupole Splitting (QS) of the Fe atoms in all sites of the 1:12 lattice, as referred to the data in ref [16]. The Fe occupancy in the different sites, however, remains unchanged within the experimental error. The increase of Bhf correlates with the changes of magnetization and Curie temperature in the nitrogenated samples. Changes in QS are in the basis of the anisotropy increase upon nitrogenation.

Table 2: *Mössbauer parameters for nitrogenated $Nd_{0.6}Zr_{0.4}Fe_{10}Si_2$. Selected values of the non-nitrogenated compound, taken from ref. [16], are in brackets.*

Phase (% Fe)	Fe position	% Fe[a] (norm)	ISO[b] (mm/s)	QS (mm/s)	B_{hf} (T)	WID (mm/s)
1:12 (89%)	8i	39	-0.01	-0.11 [0.27]	26.0 [24.3]	0.81
	8j	36	0.19	0.39 [0.16]	25.2 [22.5]	0.49
	8f	25	0.11	0.09 [-0.25]	21.9 [21.6]	0.38
bcc Fe-Si (11%)	A8	41	0.04	0.00	33.0	0.36
	A7	59	0.08	0.00	30.8	0.36

[a] Normalized to the total Fe in the corresponding phase, [b] Relative to the calibration Fe foil

a) Spark Plasma Sintering

Spark Plasma Sintering, SPS, was performed in sample A1 (100% N) at different temperatures around the expected decomposition range (550-700ºC). 8 mm diameter WC dies were used in al cases at pressures of 300 and 400 MPa (table 2), depending on the sintering temperature. Reducing the time of the thermal treatment to a few minutes, is expected to retain the nitrogen and hinder the phase segregation during sintering, at temperatures above 500ºC. Therefore, heating was programmed to last 7 min., starting after the application of pressure at RT and to stay at the maximum temperature for only 1 minute before cooling to RT at the same rate as heating. The displacement of the upper piston (Δ) and its time derivative (*dΔ/dt*) were recorded during all treatment (figure 5).

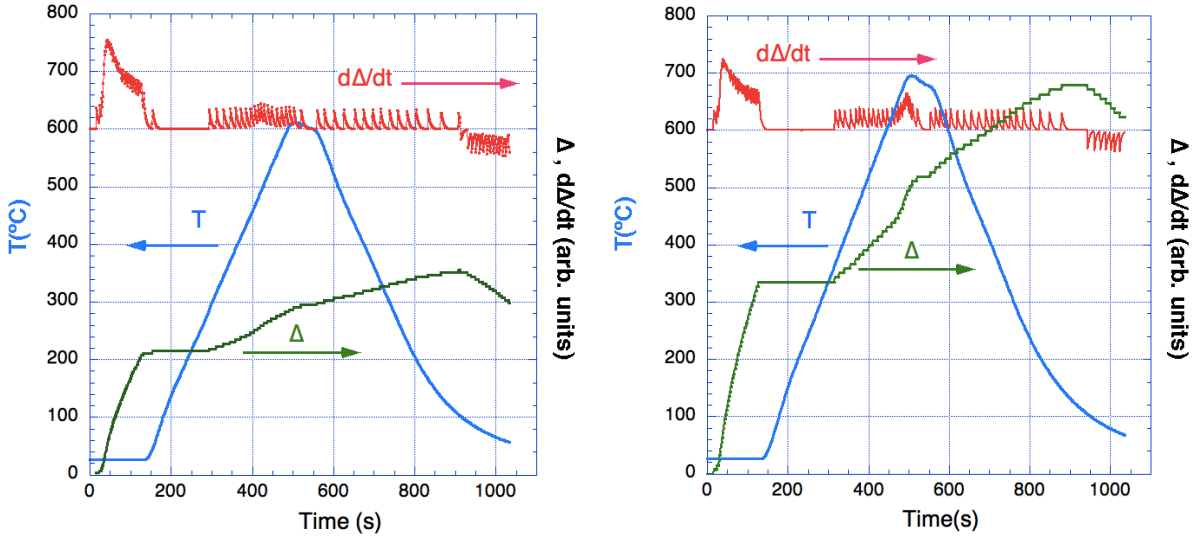

Figure 5.- *SPS records of two samples heated up to 600ºC (left) and 680ºC (right) for 1 min., showing a new process appearing at about 650ºC (500 seconds) in the second case. The displacement (Δ) and its derivative (dΔ/dt) are displayed in arbitrary units, scaled and displaced as to fit into the graphic.*

For sintering temperatures up to 600ºC, the displacement shows a monotonous behavior of volume reduction under pressure and temperature. Above 600ºC there is a new process, as disclosed by the anomaly in the displacement and its derivative around 600-650ºC (Figure 5 right). Magnetic TGA reveals a single Tc between room temperature and 500ºC in all sintered samples (Figure 6), which is well above the Tc of the powder before nitrogenation, indicating a homogeneously nitrogenated phase in all SPS samples. The sample sintered at 560ºC was not fully compacted and broke spontaneously in many pieces after manipulation. The samples sintered at higher temperatures are fully compacted although quite brittle, and must be manipulated with care.

The Tc of the samples sintered at 560 and 600ºC is even higher than that of the nitrogrenated

powder, but it decreases rapidly for SPS above 600ºC. The same happens with the coercivity, that increases first and drops above 600ºC.

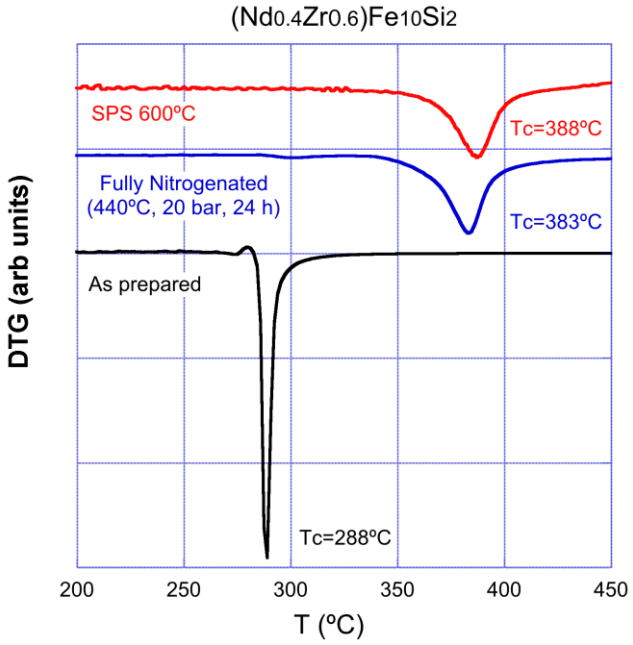

Figure 6.- *Tc of the as milled powder (lower), nitrogenated (middle) and sintered sample A1-1 (upper) of* $Nd_{0.4}Zr_{0.6}Fe_{10}Si_2(N)$ *determined by magnetic TGA. Only the derivatives of the apparent weight curve are shown for clarity. A single Tc is present in all the scanned range, confirming the full nitrogenation of the compound even after SPS at 600ºC.*

The transformation of the samples above 600ºC has been followed by XRD (Figure 7 left). They do not show any definite trend in lattice parameters upon sintering, either for the 1:12 phase or for the Fe-Si one. Therefore, the composition of the Fe-Si and the 1:12 phases, remain almost unchanged. Some relative intensity changes hint for a partial redistribution of the atoms in the unit cell. The quality of the spectra and the very broad peaks, however, do not allow an accurate determination of the atomic occupations. Above 600ºC the segregation of Fe-Si proceeds very rapidly (table 2). No new crystalline phases are shown in the patterns, although broad bumps appear in various positions in the background. The increase of bcc Fe-Si is in the basis of a rapid degradation of the magnetic hardness. In a parallel way, low field magnetization increases as the Fe-Si phase growths (fig. 7 right)

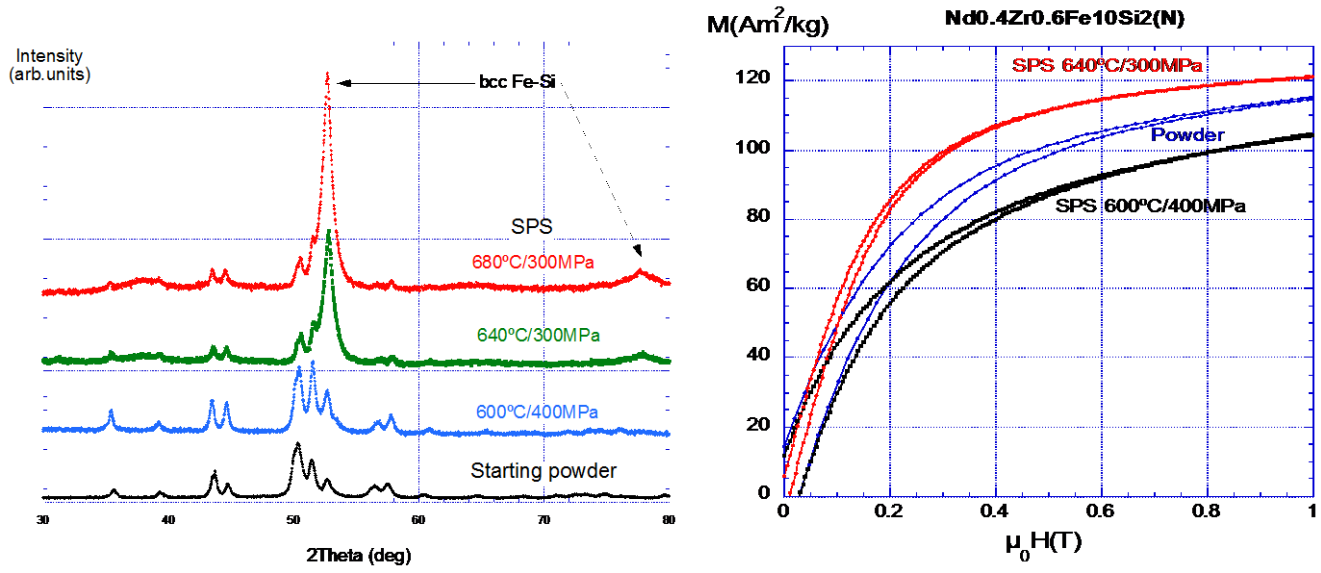

Figure 7.- *Left: Co-Kα room temperature XRD of the starting powder and spark plasma sintered samples of $Nd_{0.4}Zr_{0.6}Fe_{10}Si_2(N)$, showing the segregation of α-Fe-Si at high temperatures, as evidenced by the increase of the bcc Fe-Si peaks. Right: Magnetization curves of the initial powders and selected SPS samples*

A summary of the parameter evolution along the SPS process at different temperatures is shown in table 3. The most noticeable result is the slight improvement of magnetic properties at low temperature SPS, as compared with the starting nitrogenated powder. Fine tuning of the sintering conditions is still needed to take the best advantage of the technique.

Table 3: *Summary of the SPS experiments on $Nd_{0.6}Zr_{0.4}Fe_{10}Si_2$ (N) and the magnetic properties achieved (All treatments performed in 8mm diameter WC dies)*

Nº	Temperature / time	Pressure (MPa)	μ_0Hc (mT)	M[a] (Am^2/kg)	Tc (ºC)	α-Fe-Si (%)
Starting powder			22	115	383	12[b], 11[c]
A1-4	560ºC/1min	400	29	105	395	-
A1-1	600ºC/1min	400	27	104	388	37[b]
A1-2	640ºC/1min	300	9	121	366	73[b]
A1-3	680ºC/1min	300	6	133	341	87[b]

[a] Measured at 1 Tesla, [b] from XRD, [c] from Mössbauer

Conclusions

Our studies conclude that nitrogenation of $(NdZr)Fe_{10}Si_2$ is possible at high nitrogen pressures which leads to a large improvement of their magnetic properties, even at low nitrogen contents. Spark plasma sintering is appropriate for sintering metastable materials such as $(NdZr)Fe_{10}Si_2$

into compact material without losing the functional properties. In particular SPS below 600ºC for 1 min keeps all the nitrogen into the original compound and maintains the 1:12 structure and magnetic properties without undergoing segregation of α-Fe-Si and loss of magnetic hardness. The degradation of properties only happens above 600ºC. The studied compounds are very likely candidates for a new generation of RE lean permanent magnets, because of its Nd content of only 3-4.6 at.%.

Acknowledgments

The authors wish to acknowledge Profs. N. Randrianantoandro and E. Devlin for fruitful discussions about the fitting of the Mössbauer spectra. This work has received funding from the European Union's Horizon 2020 research and innovation program under grant agreement No 686056 (NOVAMAG) and from USA DOE grant No BES-DE-FG02-90ER45413. One of us (JMB) acknowledges a mobility fellowship of the Basque Government (grant nº MV-2018-1-0030) for his stay at the Laboratoire SATIE, ENS Paris-Saclay.

References

[1] "Tackling the challenges in commodity markets and on raw materials", COM. (2011) 25.

[2] J.M.D. Coey, "Permanent magnets: Plugging the gap", *Scr. Mater*. **67** (2012) 524–529.

[3] K.H.J. Buschow, "Permanent magnet materials based on tetragonal rare earth compounds of the type $RFe_{12-X}M_X$", *J. Magn. Magn. Mater*. **100** (1991) 79–89

[4] K H J Buschow: "New developments in hard magnetic materials", *Rep. Prog. Phys.* **54** (1991) 1123

[5] G. C. Hadjipanayis. Z. Wang. W. Singleton. B. Yelon: "Rare-earth nitrides and carbides: A new class of permanent magnet materials". *Journal of Materials Engineering and Performance*, **1**, (2) 193–203 (1992)

[6] D. Goll, R. Loeffler, R. Stein, U. Pflanz, S. Goeb, R. Karimi, G. Schneider, "Temperature dependent magnetic properties and application potential of intermetallic $Fe_{11-X}Co_XTiCe$", *Phys. Status Solidi - Rapid Res. Lett*. **8** (2014) 862–865.

[7] C. Zhou, F.E. Pinkerton, J.F. Herbst, "High Curie temperature of Ce–Fe–Si compounds with $ThMn_{12}$ structure", *Scr. Mater.* **95** (2015) 66–69.

[8] C. Zhou, K. Sun, F.E. Pinkerton, M.J. Kramer, "Magnetic hardening of

$Ce_{1+X}Fe_{11-Y}Co_YTi$ with $ThMn_{12}$ structure by melt spinning", *J. Appl. Phys*. **117** (2015) 17A741.

[9] A.M. Gabay, A. Martín-Cid, J.M. Barandiaran, D. Salazar, G.C. Hadjipanayis, "Low-cost Ce_{1-X} $Sm_X(Fe, Co, Ti)_{12}$ alloys for permanent magnets", *AIP Adv*. **6** (2016) 56015.

[10] A. Martin-Cid, D. Salazar, A.M. Schönhöbel, J.S. Garitaonandia, J.M. Barandiaran, G.C. Hadjipanayis, "Magnetic properties and phase stability of tetragonal $Ce_{1-X}Sm_XFe_9Co_2Ti$ 1:12 phase for permanent magnets", *J. Alloys Compd.* **749** (2018) 640–644.

[11] K.H.J. Buschow, "Structure and magnetic properties of some novel ternary Fe- rich rare-earth intermetallics", *J. Appl. Phys.* **63** (1988) 3130-3135.

[12] K. Ohashi, Y. Tawara, R. Osugi, M. Shimao, "Magnetic properties of Fe-rich rare-earth intermetallic compounds with a $ThMn_{12}$ structure", *J. Appl. Phys*. **64** (1988) 5714-5716.

[13] P. Stefanski, A. Werzeciono, "Structural and magnetic properties of RFe10Si2 compounds", *J. Magn. Magn. Mater*. **82** (1989) 125-128.

[14] A.M. Gabay, G.C. Hadjipanayis, "ThMn12-type structure and uniaxial magnetic anisotropy in $ZrFe_{10}Si_2$ and $Zr_{1-X}Ce_XFe_{10}Si_2$ alloys" . *J. Alloys Compd*. **657** (2016) 133-137.

[15] D. Salazar, A. Martín-Cid, J.S. Garitaonandia, T.C. Hansen, J. M. Barandiaran, G. C. Hadjipanayis, "Role of Ce substitution in the magneto-crystalline anisotropy of tetragonal $ZrFe_{10}Si_2$" *J. Alloys Compd.* **766** (2018) 291-296

[16] M. Gjoka, V. Psycharis, E. Devlin, D. Niarchos, G. Hadjipanayis, "Effect of Zr substitution on the structural and magnetic properties of the series $Nd_{1-X}Zr_XFe_{10}Si_2$ with the $ThMn_{12}$ type structure", *J. Alloys Compd*. **687** (2016) 240-245

[17] S. Sakurada, A. Tsutai, M. Sahashi, "A study on the formation of $ThMn_{12}$ and $NaZn_{13}$ structures in $RFe_{10}Si_2$", *J. Alloys Compd*. **187** (1992) 67e71

[18] A. Aubert, V. Loyau, F. Mazaleyrat, M. LoBue, "Uniaxial anisotropy and enhanced magnetostriction of $CoFe_2O_4$ induced by reaction under uniaxial pressure with SPS", *Journal of the European Ceramic Society*, **37** (2017) 3101–3105

[19] W. Q. Liu, Z. Z. Cui, X. F. Yi, M. Yue, Y. B. Jiang, D. T. Zhang, J. X. Zhang, and X. B. Liu, "Structure and magnetic properties of magnetically isotropic and anisotropic Nd–Fe–B permanent magnets prepared by spark plasma sintering technology"; *Journal of Applied Physics* **107**, 09A719 (2010)

[20] N V Rama Rao, P Saravanan, R Gopalan, M Manivel Raja, D V Sreedhara Rao, D Sivaprahasam, R Ranganathan and V Chandrasekaran, "Microstructure, magnetic and Mössbauer studies on spark-plasma sintered Sm–Co–Fe/Fe(Co) nanocomposite magnets", J. Phys. D: Appl. Phys. **41**, 065001 (2008)

[21] J Kong, C Zhou, F E Pinkerton, "Magnetic Properties of Interstitially Modified Ce-Nd-Fe-Mo-N Magnets Prepared by Spark Plasma Sintering", IEEE Trans. on Magn. **52** (7)

2100704 (2016)

[22] J. M. D. Coey, "Interstitial intermetallics", J. Magn. Magn. Mater. **159** (1–2), 80-89 (1996).

[23] G. Zougenelis, M. Aragnostou and D. Niarchos, "Mössbauer and magnetic studies of the Lu2Fe17Nx, Sm2Fe17Nx intermetallic compounds", Solid State Comm, **77** (1) 11-16 (1991)

[24] M. Fallot, "Ferromagnétisme des alliages de fer" Ann. Physique, **11** (6) 305-387 (1936)

[25] N. Randrianantoandro, E. Gaffet, J. Mira and J-M. Greneche, Solid State Commun. **111**, 323 (1999)

Supplementary material: MagneticAnisotropy of the nitrogenated compound $Nd_{0.4}Zr_{0.6}Fe_{10}Si_2(N)$

A) XRD of oriented powders

X-Ray diffraction using CuKa radiation shows almost perfect orientation along the c axis (002 direction) and, therefore, the uniaxial character of the anisotropy

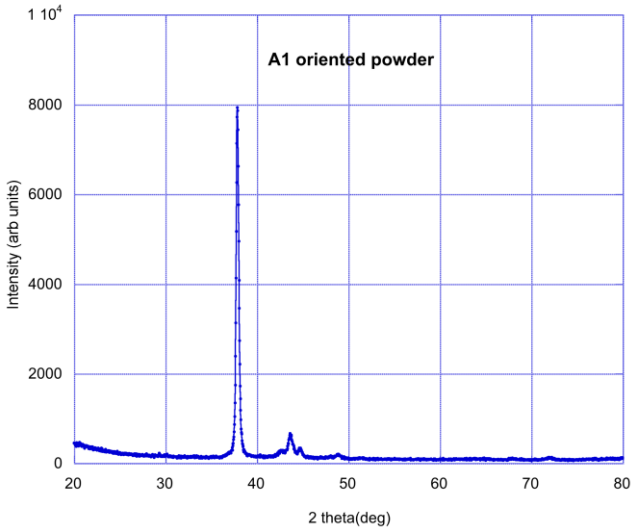

B) Fitting of the magnetization curve of oriented powder to two anisotropy constants

Fit nº1: Perfect pseudo-crystal

Calculation of the demagnetization curve from 5 T to 0 T, with H perpendicular to easy axis

Refined parameters:

$K_1 = 410\ kJm^{-3}$, $K_2 = 770\ kJm^{-3}$

$\mu oMsH^K = 2\ K_1 + 4\ K_2 = 3900\ kJm^{-3}$

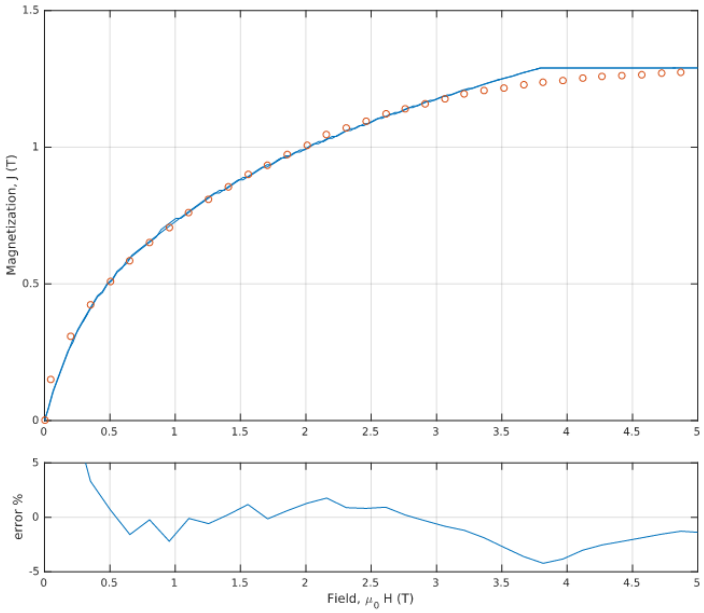

Fit nº2: Anisotropic powder with some dispersion
Identical principle but with Gaussian distribution (standard deviation σ) of easy axes around the averaged easy axis and tilt angle of the sample (θ) with respect to the perpendicular of the field. A possible distribution of the magnitude of the anisotropy constants can give similar results.

Refined parameters:
K_1= 616 kJm^{-3}, K_2= 642 kJm^{-3}
σ = 5.15°, θ = 2°
μoMsH^K= 2 K_1 + 4 K_2 = 3750 kJm^{-3}

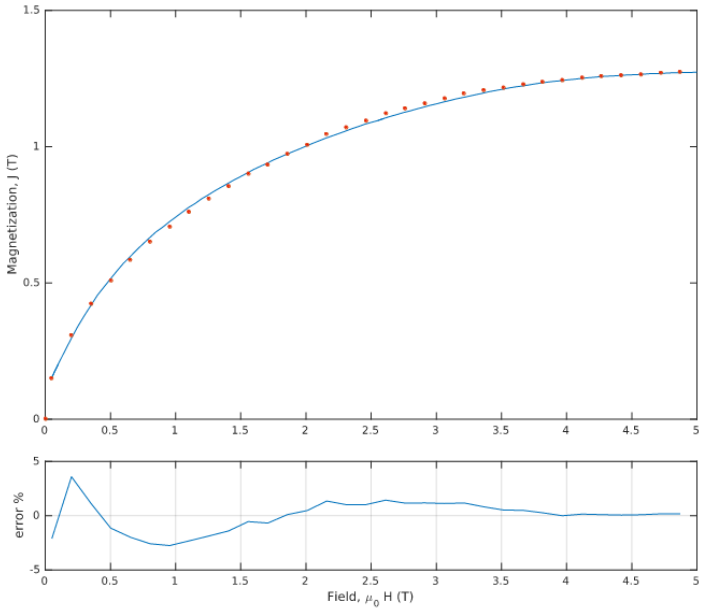

Conclusion: The material exhibits a perpendicular magnetization curve with strong positive K_1 and K_2, so it is clearly an easy axis material.
Introduction of a distribution of easy axes smooths the curve in the approach to saturation and - together with he tilt – gives rise to a small remanence. The dispersion of easy axes affects the values of K_1 (larger) and K_2 (smaller), as compared to the perfect pseudo-crystal approach, but the final H^K is very similar.